Coded *M*-ary Pulse Position Modulation for Transmitted Reference UWB Communication System

M. Herceg[1], J. Milanovic[2], M. Vranjes[1]
[1]*Department of Communications, Faculty of Electrical Engineering Osijek, Osijek 31000, Croatia*
[2] *Croatian Post and Electronic Communication Agency, Zagreb 10110, Croatia*
josip.milanovic@hakom.hr

***Abstract*—In this paper, a coded *M*-ary pulse position modulation (PPM) scheme for transmitted reference ultra-wideband (TR-UWB) systems is proposed. In conventional *M*-ary PPM TR-UWB scheme, modulation level *M* is defined only with a number of possible pulse positions *Z*. So, *Z* radio frequency (RF) wideband delay lines are required in order to map data bits into the proper pulse position, which makes such system very impractical to implement when the current CMOS technology is used. In the proposed scheme the number of required delay lines is reduced by mapping data bits in both, pulse position and *K* different orthogonal codes on frame level of the signal, producing a modulation level of *M* = *KZ*. To evaluate the performances of the proposed coded *M*-ary PPM scheme, the analytical model for realistic IEEE standard UWB channel models is developed. The performances of the proposed scheme are compared with these of the conventional *M*-ary PPM scheme for the same modulation level *M*. The results show that the proposed coded *M*-ary PPM scheme achieves approximately the same bit error probability (BEP), higher data rate and higher bandwidth efficiency, while the hardware complexity is lower in terms of number of required RF delay lines. However, by increasing the number of used orthogonal codes the minimum number of frames per one information symbol rises and consequently the maximum achievable data rate is limited. Thus the trade-off between the number of orthogonal codes and target data rate should be made.**

***Index Terms*—IEEE802.15.3a, inter symbol interference (ISI), modulation coding, ultra wideband technology (UWB).**

I. INTRODUCTION

There are many challenges that emerge in development of the short range, high speed communication systems. Although ultra-wideband (UWB) technology is not a new technology, high data rate, high channel capacity, coexistence with other technologies, outstanding multipath performances and interference immunity make it attractive solution for industry and research community. UWB technology is characterized by very low effective radiated power and extremely low power spectral density. For data transmission UWB technology uses very short pulses which are shorter than 2 ns. The usage of the short pulses results in wide spectrum occupancy while the lower power ensures avoidance of interference between UWB signals and signals from other wireless technologies which use the same frequency band.

UWB enables the usage of various modulation types, including on-of keying (OOK) [1], pulse amplitude modulation (PAM) [2], bi-phase shift keying (BPSK) [3], pulse position modulation (PPM) [4], pulse interval modulation (PIM) [5] as well as different hybrid modulation schemes which improves system performances [6], [7]. According to system complexity constraints and performance requirements, different receiver types are developed, e.g. Rake receiver and transmitted reference (TR) receiver. Due to the rich multipath signal propagation in UWB channels, the Rake receiver is needed when coherent systems have to be implemented [8]. At the Rake receiver, the channel estimation is required in order to demodulate the received signal. This is a very difficult and hardware demanding task. To overcome this limitation, in [9] TR non-coherent system was proposed. When TR scheme is used, despite the channel distortions and multipath propagation, the channel estimation is not required at the receiver in order to make a proper demodulation.

In a TR scheme, data is carried with two pulses; one, known as the reference pulse, is unmodulated and the other one is time delayed data modulated pulse, known as the data pulse. If the time delay between the reference and the data pulse is less than the channel coherence time, both pulses experience the same channel conditions and hence the reference pulse can be used as the template signal needed for correlation with the data pulse at the receiver. Then the channel estimation at the receiver is avoided, which significantly reduces hardware complexity.

However, the main drawbacks of the TR receiver are performance degradation due to the usage of noisy template waveform (which degrades the system performance) and usage of RF wideband delay lines (which are very difficult to implement in current CMOS technology). The data rate and power efficiency are also double decreased due to the transmitting of the reference pulse. The situation is even worse if it is taken into account that, in order to avoid the

Manuscript received March 28, 2014; accepted September 15, 2014.

inter pulse interference (IPI) between the reference and the data pulse, delay of the data pulse should be larger than the channel delay spread (T_{mds}). That additionally limits data rate capabilities, since channel delay spread of UWB signals can be quite large [10]. To cancel the IPI and to increase the data rate, a balanced TR signalling scheme was proposed in [11]. The scheme proposed in [11] eliminates IPI by using a pair of matched-filters, which allows smaller time delays (less than T_{mds}) between the reference and the data pulse and hence the data rate is increased. In [12] *M*-ary TR PPM scheme was proposed, in which the data rate was increased by increasing modulation level *M*. However, that scheme requires $M = Z$ RF wideband delay lines in order to form the appropriate symbol. In this paper the coded *M*-ary TR PPM scheme is proposed, in which the number of required delay lines is reduced by mapping data bits in both, pulse position and *K* different orthogonal codes on frame level of the signal. For the proposed scheme the modulation level *M* is equal to *KZ*, and *K* times less RF wideband delay lines are required for the same modulation level *M*, compared to the conventional *M*-ary TR PPM scheme. Furthermore, by using the proposed scheme the data rate is increased by reducing the number of RF wideband delay lines (shorter frame time), which also increases the bandwidth efficiency when comparing to the conventional *M*-ary TR PPM system. Although this paper deals only with the single user scenario, the multiple access techniques such as time-hoping or spreading sequence can be used along with this scheme.

The paper is organized as follows. In Section II, the analysed coded *M*-ary PPM TR-UWB scheme is described in its three main components, the transmitter, the channel model and the receiver. Section III gives the performance analysis of the proposed coded *M*-ary PPM TR system, while the simulation and numerical results are presented in Section IV. Concluding remarks are given in Section V.

II. SYSTEM MODEL

A. Transmitted Signal

In conventional *M*-ary TR PPM scheme the transmitted signal consists of the reference and the time delayed data modulated pulse, where the time delay is determined by the proper data which is sent. The transmitted signal of the *i*-th symbol can be written as

$$s_i(t) = \sqrt{\frac{E_s}{2N_s}} \sum_{j=iN_s}^{(i+1)N_s-1} \Big(p(t - jT_f) + p\big(t - jT_f - T_d - d_i\Lambda\big)\Big), \quad (1)$$

where E_s is energy used for transmitting of one symbol, $p(t)$ is the transmitted pulse waveform with duration T_p and unit energy, $\int_{-\infty}^{\infty} p^2(t)dt = 1$, while T_f denotes frame time. N_s is the number of frames used to transmit one information symbol. Then the overall symbol duration is $T_s = N_s T_f$. Minimum time delay between the reference and the data pulse is denoted by T_d, $d_i \in \{0,1,...Z-1\}$ represents the *i*-th transmitted symbol pulse position $\left(i = \lfloor j / N_s \rfloor\right)$ and *Z* represents the number of possible pulse positions. For the conventional *M*-ary TR PPM scheme the modulation level *M* is equal to *Z* ($M = Z$). Λ denotes the data pulse time shift associated with the PPM scheme, that should be at least equal to $T_d = T_{mds}$ in order to avoid IPI. According to that, the conventional *M*-ary PPM scheme needs *M* RF wideband delay lines, which significantly increases the hardware complexity and reduces the data rate (due to the larger symbol duration).

In order to increase the data rate and to improve the bandwidth efficiency, the coded *M*-ary PPM scheme, which reduces the number of needed RF wideband delay lines, is presented. In coded *M*-ary PPM scheme the transmitted signal of the *i*-th symbol can be written as

$$s_i(t) = \sqrt{\frac{E_s}{2N_s}} \sum_{j=iN_s}^{(i+1)N_s-1} \Big(p(t - jT_f) + (-1)^{\left\lfloor \frac{j}{2^{k_i}} \right\rfloor} p(t - jT_f - T_d - d_i\Lambda)\Big), \quad (2)$$

where $\lfloor \bullet \rfloor$ is the integer floor operator and $k_i \in \{0,1,...K-1\}$ determines the *i*-th transmitted symbol unique orthogonal code. The properties of the codes defined in (2) are:

$$\sum_{j=iN_s}^{(i+1)N_s-1} (-1)^{\left\lfloor \frac{j}{2^{k_i}} \right\rfloor} = 0, \text{ for any } k_i, \quad (3)$$

$$\sum_{j=iN_s}^{(i+1)N_s-1} (-1)^{\left\lfloor \frac{j}{2^{r}} \right\rfloor} (-1)^{\left\lfloor \frac{j}{2^{p}} \right\rfloor} = \begin{cases} N_s, & \text{when } r = p, \\ 0, & \text{when } r \neq p, \end{cases} \quad (4)$$

where $r \in \{0,1,...K-1\}$ and $p \in \{0,1,...K-1\}$.

The relationship between N_s and the number of possible codes *K* is $N_s = 2^K$, which means that N_s has to be set as a power of 2 in order to achieve the orthogonality between different codes over the symbol period [11]. Due to the fact that information is mapped in both the unique orthogonal code and the pulse position, the number of bits per symbol, *b*, in coded *M*-ary PPM scheme is equal to $b = \log_2(M) = \log_2(KZ)$. Then for the same modulation level *M* (the same number of bits per symbol) the proposed scheme requires *K* times less RF wideband delay lines than the conventional *M*-ary TR PPM scheme. For example, supposing that in both schemes (conventional and coded *M*-ary PPM scheme) the modulation level is set to $M = 8$ and the number of possible codes in coded *M*-ary PPM scheme is $K = 2$, then the proposed scheme requires two times less RF wideband delay lines ($Z = 4$) then the conventional scheme ($Z = 8$). The data rate is then double increased (the symbol duration is double decreased), while hardware complexity is significantly reduced. In general the data rate is given by

$$R_b = \frac{\log_2(M)}{N_s T_f}. \quad (5)$$

In order to avoid the inter-frame interference (IFI) and inter-symbol interference (ISI), minimum T_f for the conventional *M*-ary TR PPM scheme is given by

$$T_f = (2M+1)T_{mds}, \tag{6}$$

while for the proposed coded *M*-ary TR PPM scheme minimum T_f is defined as

$$T_f = (2\frac{M}{K}+1)T_{mds}, \tag{7}$$

resulting with data rate increasing due to decreasing of frame duration.

B. UWB Channel Model

Unlike narrowband systems, where the fading can be considered as a frequency-flat, in UWB systems fading must be considered as a highly frequency-selective because of the large bandwidth that UWB pulses occupy (around 7.5 GHz). Therefore it was necessary to develop the appropriate channel model for the proper physical layer analysis of UWB systems.

From [13] it can be seen that in UWB channel the multipath components tend to arrive in clusters, and fading for each cluster as well as for each ray within the cluster is different. Neglecting the shadowing effects, the channel impulse response can be expressed as

$$h(t) = \sum_{l_c=1}^{L_c}\sum_{l_r=1}^{L_r} \sim_{l_c,l_r} \delta(t - T_{l_c} - \text{²}_{l_c,l_r}), \tag{8}$$

where $\sim_{l_c,l_r}$ is the gain coefficient of the l_r-th multipath component in the l_c-th cluster, $\delta(.)$ is the Dirac delta function, T_{l_c} is the l_c-th cluster arrival time, $\text{²}_{l_c,l_r}$ is the delay of the l_r-th multipath component relative to the T_{l_c}, L_c and L_r are the total number of clusters and the total number of multipath component within each cluster, respectively.

Based on the measurements that have been made, the IEEE 802.15.3a working group defined four types of indoor wireless channel models. The details about these channel models can be found in [13].

In this work discrete channel models CM1 and CM3 are used, where CM1 corresponds to the line-of-sight (LOS) propagation conditions and CM3 corresponds to the non-line-of-sight (NLOS) propagation conditions. In these channel models the whole signal arrival time is divided into time bins with duration Δ = 0.167 ns, as in [11], [14]. In order to avoid IPI, in this work the duration of the transmitted pulse is set to T_p = 0.167 ns [11], [14], [15]. Discrete-time channel impulse response presented with (8) can be simplified and written as

$$h(t) = \sum_{l=1}^{L_p} \sim_l \delta(t - l\Delta), \tag{9}$$

where $\sim_l$ is the sum of the gain coefficients of all multipath components arrived in the *l*-th time bin. $L_p = L_c L_r$ is the total number of multipath components, $l\text{a}$ is delay of the *l*-th time bin relative to the first time bin. Hence, the channel delay spread will be equal to $T_{mds} = L_p\text{a}$.

C. Receiver Processing

After propagation through UWB channel, a single-user coded *M*-ary TR PPM signal is mixed with additive white Gaussian noise (AWGN), resulting with the signal-to-noise ratio (SNR) reduction at the receiver. The received signal of the *i*-th symbol can be expressed as the convolution of the transmitted signal and the channel impulse response

$$\begin{aligned} r_i(t) &= h(t) \otimes s_i(t) + n(t) = s_{r,i}(t) + n(t) = \\ &= \sqrt{\frac{E_s}{2N_s}} \sum_{j=iN_s}^{(i+1)N_s-1} \Big(g(t - jT_f) + \\ &+ (-1)^{\left\lfloor \frac{j}{2^{k_i}} \right\rfloor} g(t - jT_f - T_d - d_i\Lambda) \Big) + n(t), \end{aligned} \tag{10}$$

where

$$g(t) = h(t) \otimes p(t) = \sum_{l=1}^{L_p} \sim_l p(t - l\Delta), \tag{11}$$

is the received waveform and $\otimes$ denotes the convolution operator. $n(t)$ is a filtered AWGN with power spectral density (PSD) of $N_0/2$.

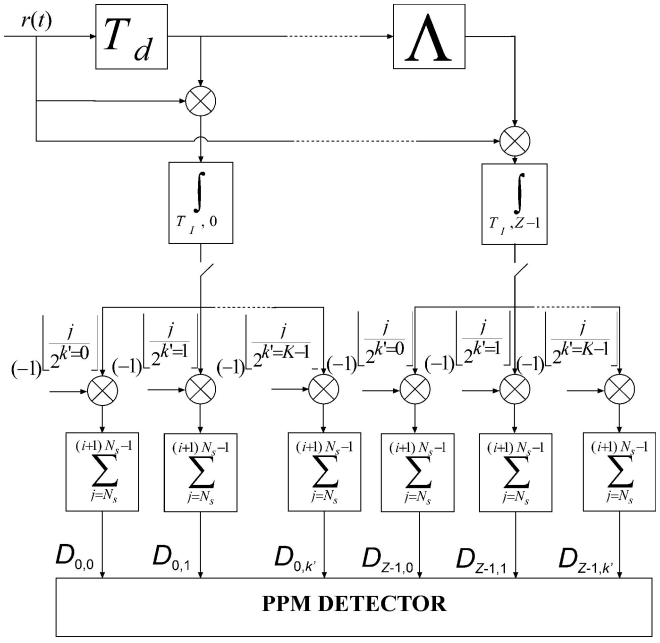

Fig. 1. Coded *M*-ary TR PPM receiver structure.

In Fig. 1 the receiver for the proposed coded *M*-ary TR PPM scheme is shown. At the receiver, the correlation between the reference pulse and the appropriate data pulse is performed, producing *Z* correlation outputs related to the pulse positions.

Each output is then divided into *K* branches, and in each branch the correlation output is then multiplied for each

frame by one of the $(-1)^{\lfloor j/2^{k'} \rfloor}$ orthogonal codes, where parameter $k' \in \{0,1,...K-1\}$ defines the unique orthogonal code at the receiver side. The decision variable for the i-th symbol at the z-th position coded by the k'-th code (z,k') can be expressed as

$$D_{z,k',i} = \sum_{j=iN_s}^{(i+1)N_s-1} (-1)^{\left\lfloor \frac{j}{2^{k'}} \right\rfloor} \int_{T_{I,z}} r_i(t) r_i(t - T_d - z\Lambda) dt, \quad (12)$$

where $z \in \{0,1,...Z-1\}$ and $T_{I,z}$ is the z-th position integration time defined as

$$T_{I,z} = \left(jT_f + T_d + z\Lambda, jT_f + T_d + z\Lambda + T_{corr} \right). \quad (13)$$

Correlation time is assumed to be an integer multiple of the pulse width, denoted as $T_{corr} = L_{corr}T_p \le T_{mds}$, where $L_{corr} \in \{1,2,\ldots,L_p\}$. After demodulation, based on expression (12) the receiver compares the values of $\left\{D_{z,k',i}\right\}_{z=0,\,k'=0}^{Z-1,\,K-1}$ and chooses the output with the largest magnitude in order to detect the position the pulse is sent in and the code it is coded by.

III. PERFORMANCE ANALYSIS

A disadvantage of the TR receiver comparing to Rake receiver is in certain amount of performance degradation. Since "noisy" reference pulse is used as a template signal for the correlation process, the frame's correlation outputs $D_{z,k',i}$ from (12) contain a *signal* × *noise* component which additionally degrades system performances.

To perform the system performance analysis, without loss of generality it can be assumed that the data pulse is transmitted in the first position ($z = 0$) coded by the k_i-th code in the i-th symbol. The decision variable from (12) $D_{z,k',i}$ can be rewritten as

$$D_{z,k',i} = \begin{cases} £_{k',i} + N_{z,k',i,1} + N_{z,k',i,2}, & \text{for } z = 0; \text{ any } k', \\ N_{z,k',i,1} + N_{z,k',i,2}, & \text{for } z \ne 0; \text{any } k', \end{cases} \quad (14)$$

where $£_{k',i}$ is a desired signal, $N_{z,k'i,,1}$ is a *signal* × *noise* component and $N_{z,k',i,2}$ is a *noise* × *noise* component. Desired signal $£_{k',i}$ can be calculated as

$$£_{k',i} = \int_{T_{I,z}} s_{r,i}(t) s_{r,i}(t - T_d) dt =$$

$$= \sum_{j=iN_s}^{(i+1)N_s-1} \frac{E_s}{2N_s} \left[(-1)^{\left\lfloor \frac{j}{2^{k'}} \right\rfloor} \int_{T_d}^{T_d+T_{corr}} g(t) g(t - T_d) dt + \right.$$

$$+ (-1)^{\left\lfloor \frac{j}{2^{k_i}} \right\rfloor} (-1)^{\left\lfloor \frac{j}{2^{k'}} \right\rfloor} \int_{T_d}^{T_d+T_{corr}} g(t) g(t - 2T_d) dt +$$

$$+ (-1)^{\left\lfloor \frac{j}{2^{k_i}} \right\rfloor} (-1)^{\left\lfloor \frac{j}{2^{k'}} \right\rfloor} \int_{T_d}^{T_d+T_{corr}} g^2(t - T_d) dt +$$

$$\left. + (-1)^{2\left\lfloor \frac{j}{2^{k_i}} \right\rfloor} (-1)^{\left\lfloor \frac{j}{2^{k'}} \right\rfloor} \int_{T_d}^{T_d+T_{corr}} g(t - T_d) g(t - 2T_d) dt \right]. \quad (15)$$

In (15) the first, the second and the fourth term will be zero due to the fact that multiplication of the received waveform $g(t)$ and its time shifted version $g(t-T_d)$ will always be zero. $g(t)$, which represents a dispersed version of $p(t)$ caused by channel, has a duration of T_{mds} (according to (11)). So, by choosing that $T_{mds} \le T_d$, the upper statement will be assured. Then the (15) can be rewritten as

$$£_{k',i} = \sum_{j=iN_s}^{(i+1)N_s-1} \frac{E_s}{2N_s} (-1)^{\left\lfloor \frac{j}{2^{k_i}} \right\rfloor} (-1)^{\left\lfloor \frac{j}{2^{k'}} \right\rfloor} \times$$

$$\times \int_{T_d}^{T_d+T_{corr}} g^2(t - T_d) dt. \quad (16)$$

Furthermore, from (4) it follows

$$£_{k',i} = \begin{cases} \frac{E_s}{2} \int_{T_d}^{T_d+T_{corr}} g^2(t - T_d) dt, & \text{for any } k_i = k', \\ 0, & \text{for any } k_i \ne k'. \end{cases} \quad (17)$$

Based on (11) and (17) the mean value of the desired signal can be written as

$$E(£_{k',i}) = \begin{cases} \frac{E_s}{2} \sum_{l=1}^{L_{corr}} E(\sim_l^2) \int_0^{Tp} p^2(t) dt, & \text{for } k_i = k', \\ 0, & \text{for } k_i \ne k', \end{cases} \quad (18)$$

where $E(\sim_l^2)$ is the mean energy of the sum of the gain coefficients of all multipath components arrived in the l-th time bin defined as [11] and the overall channel energy is normalized to be $\sum_{l=1}^{L_p} E(\sim_l^2) = 1$. $E(\bullet)$ is the mean value operator.

Furthermore, the *signal* × *noise* component $N_{z,k'i,,1}$ can be written as

$$N_{z,k',i,1} = \sum_{j=iN_s}^{(i+1)N_s-1} \int_{T_d+z\Lambda}^{T_d+z\Lambda+T_{corr}} \left(n(t - T_d - z\Lambda) s_{r,i}(t) + \right.$$

$$\left. + s_{r,i}(t - T_d - z\Lambda) n(t) \right) dt. \quad (19)$$

After additional mathematical manipulation (19) can be rewritten as

$$N_{z,k',i,1} = \sum_{j=iN_s}^{(i+1)N_s-1} \sqrt{\frac{E_s}{2N_s}} \left[(-1)^{\left\lfloor \frac{j}{2^{k'}} \right\rfloor} \times \right.$$

$$\times \int_{T_d+z\Lambda}^{T_d+z\Lambda+T_{corr}} g(t)n(t-T_d-z\Lambda)dt +$$
$$+(-1)^{\left\lfloor \frac{j}{2^{k_i}} \right\rfloor}(-1)^{\left\lfloor \frac{j}{2^{k'}} \right\rfloor} \int_{T_d+z\Lambda}^{T_d+z\Lambda+T_{corr}} g(t-T_d)n(t-T_d-z\Lambda)dt +$$
$$+(-1)^{\left\lfloor \frac{j}{2^{k'}} \right\rfloor} \int_{T_d+z\Lambda}^{T_d+z\Lambda+T_{corr}} g(t-T_d-z\Lambda)n(t)dt +$$
$$+(-1)^{\left\lfloor \frac{j}{2^{k_i}} \right\rfloor}(-1)^{\left\lfloor \frac{j}{2^{k'}} \right\rfloor} \int_{T_d+z\Lambda}^{T_d+z\Lambda+T_{corr}} g(t-2T_d-z\Lambda)n(t)dt \Bigg]. \quad (20)$$

It can be easily shown that the variable $N_{z,k',i,1}$ is zero mean Gaussian random variable [16]. More detailed, in expression (20) the first and fourth term will always be zero, since the received waveform $g(t)$ will never be within the integration time, due to the fact that $T_{corr} \le T_{mds} \le T_d$. The variance of $N_{z,k',i,1}$ can be calculated as

$$\mathrm{var}\left(N_{z,k',i,1}\right) = E\left(N^2_{z,k',i,1}\right) =$$
$$= \frac{E_s N_0}{4N_s} \sum_{j=iN_s}^{(i+1)N_s-1} E\left(\int_{z\Lambda}^{z\Lambda+T_{corr}} g^2(t)dt + \int_{T_d+z\Lambda}^{T_d+z\Lambda+T_{corr}} g^2(t-T_d-z\Lambda)dt \right). \quad (21)$$

From (21) it can be seen that the variance depends only on z and can be rewritten as

$$\mathrm{var}\left(N_{z,k',i,1}\right) = E\left(N^2_{z,k',i,1}\right) =$$
$$= \begin{cases} \frac{E_s N_0}{2} \sum_{l=1}^{L_{corr}} E(\sim_l^2) \int_0^{T_p} p^2(t)dt, & \text{for } z=0 \text{ and any } k', \\ \frac{E_s N_0}{4} \sum_{l=1}^{L_{corr}} E(\sim_l^2) \int_0^{T_p} p^2(t)dt, & \text{for } z \ne 0 \text{ and any } k'. \end{cases} \quad (22)$$

Furthermore, it is assumed that $N_{z,k',i,2}$ is a Gaussian distributed random variable with zero mean and variance

$$\mathrm{var}\left(N_{z,k',i,2}\right) = \frac{N_s N_0^2 W T_{corr}}{2}, \text{ for any } z \text{ and } k', \quad (23)$$

where W is the receiver front-end filter bandwidth. The detailed derivation of the $\mathrm{var}\left(N_{z,k',i,2}\right)$ can be seen in [14].

As it is mentioned before, the detector makes a decision which symbol is sent according to the highest correlator output. So the probability that the receiver will make a correct decision when the pulse is transmitted in the first modulation position ($z = 0$) and coded by the k_i-th code can be expressed as [17], [18]

$$P_c = \int_{-\infty}^{\infty} P(D_{0,k'=k_i,i} > D_{0,k'\ne k_i,i}, D_{0,k'=k_i,i} > D_{1,k',i}, \ldots$$
$$\ldots D_{0,k'=k_i,i} > D_{Z-1,k',i} \left| D_{0,k'=k_i,i} \right) p(D_{0,k'=k_i,i}) dD_{0,k'=k_i,i}, \quad (24)$$

where $p(D_{0,k'=k_i,i})$ is the probability density function (PDF) of the first correlation output when the i-th symbol with the pulse in first position $z = 0$, coded by the k_i-th code is sent. PDF can be written as

$$p(D_{0,k'=k_i,i}) = \frac{1}{\sqrt{2\pi\, \mathrm{var}_{tot,0,k'=k_i,i}}} \times$$
$$\times \exp\left(-\frac{\left(D_{0,k'=k_i,i} - E(\xi_{k',i})\right)^2}{2\,\mathrm{var}_{tot,0,k'=k_i,i}} \right), \quad (25)$$

where $\mathrm{var}_{tot,0,k'=k_i,i}$ is the sum of all variances of the i-th symbol at the $(0, k'=k_i)$ correlator output. Assuming that all codes are equally likely and by using the same techniques as in [17], the probability of the correct decision for the i-th symbol can be calculated as

$$P_c = \frac{1}{K} \sum_{k_i=0}^{K-1} \int_{-\infty}^{\infty} \left(\prod_{z=0}^{Z-1} \prod_{\substack{k'=0, \\ \text{if } z=0 \\ k'\ne k_i}}^{K-1} \frac{1}{\sqrt{2\pi}} \times \right.$$
$$\left. \times \int_{-\infty}^{D_{0,k'=k_i,i}/\sqrt{\mathrm{var}_{tot,z,k',i}}} \exp\left(-\frac{x^2}{2}\right)dx \right) \times$$
$$\times p(D_{0,k'=k_i,i})dD_{0,k'=k_i,i}. \quad (26)$$

Finally, the probability of the symbol error is

$$P_M = 1 - P_c. \quad (27)$$

Due to the more detailed system evaluation, it is desirable to convert the probability of the symbol error into bit error probability (BEP)

$$P_b = \frac{2^{b-1}}{2^b - 1} P_M. \quad (28)$$

IV. DISCUSSION

In this section, the numerical results are presented to illustrate the proposed system performances. The IEEE 802.15.3a channel models are used [13]. The detailed results are presented for channel model CM1, while the data rate is additionally analysed for channel model CM3. The receiver filter has one-sided bandwidth W = 6 GHz, while the arrival time axis is divided into small time bins with duration of 0.167 ns, in order to eliminate IPI caused by channel distortion. Maximum channel delay spread, T_{mds}, is set to 200 time bins for CM1 (33.4 ns) and 400 time bins for CM3 (66.8 ns), what is large enough to capture most of the signal energy dispersed by the channel [14]. The transmitted energy is normalized to E_s = 1. The frame duration T_f is set to $T_f = (2M/K+1)T_{mds}$, what is large enough to ensure both,

the IFI and the ISI cancelation.

In Fig. 2 the influence of the integration time $T_{corr} = L_{corr}T_p$ on BEP performance of coded PPM scheme with $K = 2$ and $Z = 2$ in CM1 is shown. The analysis is made for different number of frames per symbol N_s and for fixed signal-to-noise ratio $E_b/N_0 = 17$ dB, where E_b is transmitted energy per bit given as $E_b = E_s/\log_2(ZK)$. As it can be seen from Fig. 2, when the integration time increases (till optimal integration time) the system performances rise because the collected desired signal energy at the receiver (see (18)) is getting higher. The optimal integration time for all analysed N_s is between 5 ns and 10 ns. However, when the integration time continues to rise (above its optimal value), the contribution of the interference components (22), (23) significantly increases and dominates over desired signal energy, resulting with the system performance degradation.

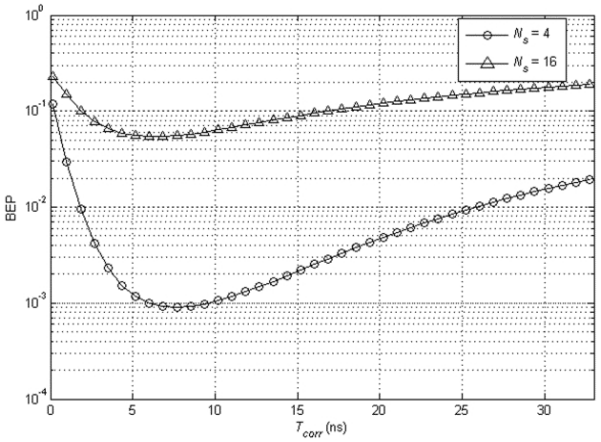

Fig. 2. The influence of the integration time T_{corr} on BEP performance of coded PPM scheme with $K = 2$ and $Z = 2$ in CM1 for different number of frames per symbol N_s.

In Fig. 3 the comparison of the conventional and the coded PPM scheme for the same modulation level in CM1 for $N_s = 16$ is shown (BEP vs. signal-to-noise ratio E_b/N_0). As it can be seen, the BEP performances are equal for both analysed schemes for the same modulation level. However, the system performances increase when the modulation level rises, what is the property of multilevel orthogonal modulation schemes. Note that the conventional PPM scheme is the special case of the proposed coded PPM scheme, when the number of used codes K is equal to 1. Thus its performances can also be obtained from expressions (25)–(28). To summarize, for the same modulation level the proposed scheme achieves approximately the same performances as the conventional one, while the hardware complexity (with regards to the number of RF delay lines) is significantly decreased.

As it is mentioned in Section II, the number of used codes, K, determines the minimal number of frames per symbol as $N_s = 2^K$. So, in Fig. 4 the performances of coded PPM scheme for the same modulation level $M = 16$, but for different combinations of K and Z are shown (for CM1). The results obtained by using numerical terms mentioned above are compared to those obtained by using Monte-Carlo simulation and the deviations are minimal. It can be seen that the coded PPM achieves the best performances for combination $K = 2$, $Z = 8$. For example, for fixed BEP of 10^{-4}, the combination $K = 4$, $Z = 4$ requires approximately 3 dB higher E_b/N_0 than the combination $K = 2$, $Z = 8$, while the combination $K = 8$, $Z = 2$ requires significantly higher E_b/N_0. Such results can be explained as follows: when the number of frames per symbol, N_s, increases, the amount of *noise*×*noise* interference rises (23), which degrades BEP performances.

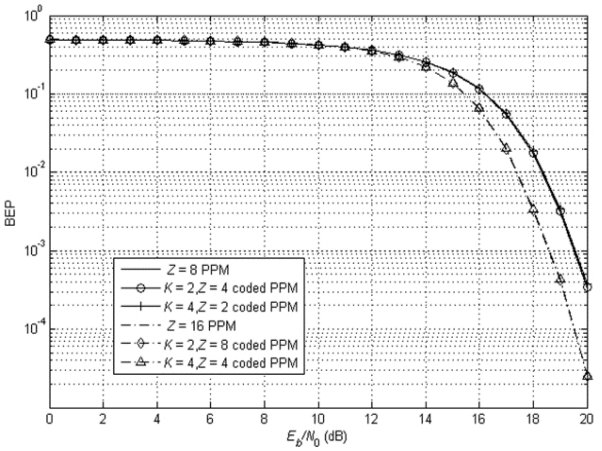

Fig. 3. The comparison of the conventional and the coded PPM scheme for modulation levels $M = 8$ and $M = 16$. Other systems parameters are $N_s = 16$, $T_{corr} = 7.515$ ns ($L_{corr} = 45$).

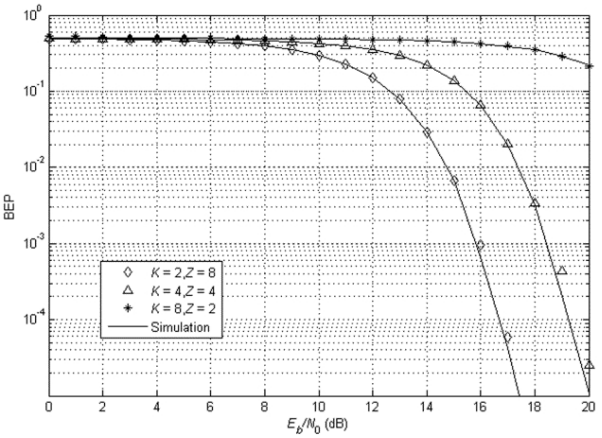

Fig. 4. The comparison of coded PPM scheme for the same modulation level $M = 16$ with different K, Z and minimal number of frames per symbol $N_s = 2^K$, $T_{corr} = 7.515$ ns ($L_{corr} = 45$).

In Fig. 5 the comparison of the conventional and the coded PPM scheme is made, with respect to the achievable bit rate for different number of frames per symbol, N_s, in CM1 and CM3.

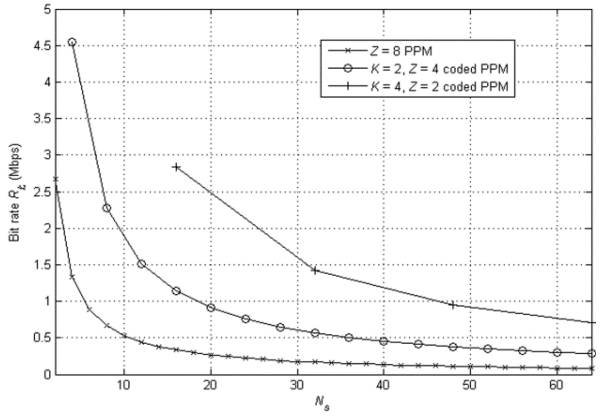

(a)

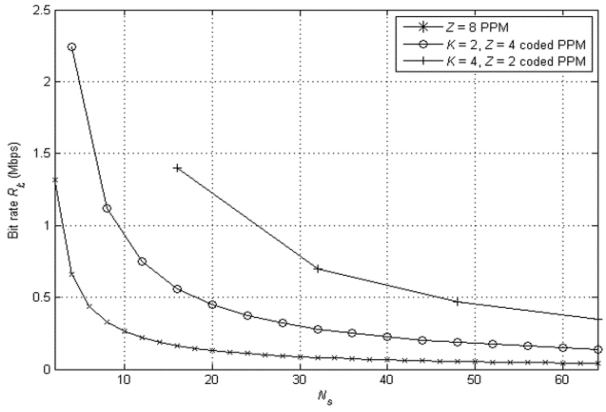

(b)

Fig. 5. The comparison of achievable data rate for the conventional and the coded PPM for (a) CM1 and (b) CM3.

As it can be seen, for fixed modulation level M = 8 the achievable bit rate increases as K rises. It comes from the fact that for higher values of K less RF delay lines are needed in order to achieve the same modulation level, and hence the frame time is shortened. For example, in CM1 (Fig. 5 a)) for N_s = 16, the bit rate is 2.8 Mbps for K = 4, Z = 2 coded PPM, while for K = 2, Z = 4 coded PPM and Z = 8 conventional PPM is 1.2 Mbps and 0.3 Mbps, respectively. Also it can be seen that the bit rate decreases as the number of frames per symbol increases, due to the longer symbol time.

The achievable bit rate for a given N_s decreases in CM3 due to the fact that channel delay spread, T_{mds}, increases to 66.8 ns and hence the minimum separation time between two pulses, T_d, rises (longer symbol duration).

V. CONCLUSIONS

In this paper a coded M-ary TR PPM scheme for UWB systems has been proposed. The proposed scheme requires K times less RF wide-band delay lines needed to map the data bits in the proper position compared to the conventional M-ary PPM scheme. That comes from the fact that, beside the position, data bits are mapped in K orthogonal codes on the frame level of the signal, which reduces the demand for hardware complexity.

It is also shown that the proposed scheme achieves approximately the same BEP performances as the conventional M-ary PPM scheme, while it significantly outperforms the conventional scheme with respect to data rate.

However, by increasing the number of used orthogonal codes the minimum number of frames per one information symbol rises and consequently the maximum achievable data rate is limited.

The balance between the BEP and data rate can be achieved by the trade-off between the system parameters like N_s, K, Z. These properties make coded PPM scheme very attractive for usage in TR-UWB communication systems.

REFERENCES

[1] L. Wei, T. A. Gulliver, "On-off keying Ultra-Wideband communication with adaptive overcomplete dictionary detection", in *2007 Proc. of Canadian Conf. on Elect. and Comput. Eng.*, pp. 1187–1190.

[2] C. J. Le Marter, G. B. Giannakis, "All-digital PAM impulse radio for multiple-access through frequency-selective multipath", in *Proc. of the IEEE Global Telecomm. Conf.*, 2000, pp. 77–81.

[3] B. Zhao, Y. Chen, R. Green, "Hard-input–hard-output capacity analysis of UWB BPSK systems with timing errors", *IEEE Trans. Veh. Technology*, vol. 61, no. 4, pp. 1741–1751, 2012. [Online]. Available: http://dx.doi.org/10.1109/TVT.2012.2188418

[4] Y. S. Shen, F. B. Ueng, J. D. Chen, S. T. Huang, "A high-capacity TH multiple-access UWB system with performance analysis", *IEEE Trans. Veh. Technology*, vol. 59, no. 2, pp. 742–753, 2010. [Online]. Available: http://dx.doi.org/10.1109/TVT.2009.2035130

[5] M. Herceg, T. Svedek, T. Matic, "Pulse interval modulation for ultra-high speed IR-UWB communications systems", *EURASIP J. Adv. Sig. Pr.*, 2010. [Online] Available: http://dx.doi.org/10.1155/2010/658451.

[6] J. Sinae, L. Sengjoo, K. Jaeseok, "Efficient hybrid modulation with phase-directed pulse position estimation for UWB-IR systems", *IEEE Trans. on Wireless Comm*, vol. 61, no. 4, pp. 1171–1177, 2013. [Online]. Available: http://dx.doi.org/10.1109/TCOMM.2013.13.110681

[7] S. Erkucuk, D. I. Kim, "M-ary code shift keying impulse modulation combined with BPPM for UWB communications", *IEEE Trans. on Wireless Comm*, vol. 6, no. 6, pp. 2255–2265, 2007. [Online]. Available: http://dx.doi.org/10.1109/TWC.2007.05803

[8] G. Durisi, S. Benedetto, "Comparison between coherent and noncoherent receivers for UWB communications", *EURASIP J. Adv. Sig. Pr.*, 2005. [Online] Available: http://dx.doi.org/10.1155/ASP.2005.359.

[9] R. T. Hoctor, H. W. Tomlinson, "An overwiev of delay–hopped transmitted-reference RF communications", in *Proc. IEEE Conf. on Ultra Wideband Syst. and Technology*, 2002, pp. 265–269.

[10] M. Z. Win, R. A. Scholtz, "Characterization of ultra-wide bandwidth wireless indoor channel: a communication-theoretic view", *IEEE J. Sel. Areas Commun.*, vol. 20, no. 9, pp. 1613–1627, 2002. [Online]. Available: http://dx.doi.org/10.1109/JSAC.2002.805031

[11] D. I. Kim, T. Jia, "*M*-ary orthogonal coded/balanced ultra-wideband transmitted-reference system in multipath", *IEEE Trans. Commun.*, vol. 56, no. 1, pp. 102–111, 2008. [Online]. Available: http://dx.doi.org/10.1109/TCOMM.2008.050310

[12] L. Li, J. K. Townsend, "*M*-ary PPM for transmitted reference ultra-wideband communications", *IEEE Trans. Commun.*, vol. 58, no. 7, pp. 1912–1917, 2010. [Online]. Available: http://dx.doi.org/10.1109/TCOMM.2010.07.080675

[13] A. F. Molisch, J. R. Foerster, M. Pendergrass, "Channel models for ultrawideband personal area networks", *IEEE Wirel. Commun.*, vol. 10, no. 6, pp. 14–21, 2003. [Online]. Available: http://dx.doi.org/10.1109/MWC.2003.1265848

[14] T. Jia, D. I. Kim, "Analysis of channel-averaged SINR for indoor UWB rake and transmitted reference systems", *IEEE Trans. Commun.*, vol. 55, no. 10, pp. 2022–2032, 2007. [Online]. Available: http://dx.doi.org/10.1109/TCOMM.2007.906435

[15] D. I. Kim, "Multiuser performance of M-ary orthogonal coded/balanced UWB transmitted-reference systems", *IEEE Trans. Commun.*, vol. 57, no. 4, pp. 1013–1024, 2009. [Online]. Available: http://dx.doi.org/10.1109/TCOMM.2009.04.070146

[16] T. Jia, D. I. Kim, "Multiple access performance of balanced UWB transmitted-reference systems in multipath", *IEEE Trans. Wireless Commun.*, vol. 7, no. 3, pp. 1084–1094, 2008. [Online]. Available: http://dx.doi.org/10.1109/TWC.2008.060864

[17] J. G. Proakis, *Digital commun*. New York: McGraw-Hill, 2001, pp. 260–264.

[18] Sang-Dong Kim, Jonghun Le1 "Design and Implementation of a Hybrid UWB Pulse Generator for Automotive Radar", *Elektronika ir Elektrotechnika*, vol. 20, no. 3, pp. 24–28, 2014. [Online]. Available: htp:/dx.doi.org/10.575/j01.ee.20.3.274